



Catalytic polymerization of ethylene in toluene using a Pd-organometallic catalyst

Sorin N. Sauca, José M. Asua*

Institute for Polymer Materials (POLYMAT) and Grupo de Ingeniería Química, Departamento de Química Aplicada, Facultad de Ciencias Químicas, University of the Basque Country, Apdo. 1072, ES-20080 Donostia-San Sebastián, Spain

ARTICLE INFO

Article history:

Received 30 April 2010

Received in revised form 19 October 2010

Accepted 20 October 2010

Keywords:

Catalytic polymerization

Ethylene

Palladium catalyst

Kinetics

Polymerization mechanism

β -Hydride elimination

ABSTRACT

The kinetics of the ethylene polymerization of ethylene in toluene using a monometallic palladium catalyst containing phosphine ligands was investigated. The effect of both external and internal mass transfer limitations was assessed. The influence of several factors (temperature, monomer concentration, catalyst concentration) on the polymerization rate, molecular weights and crystallinity was studied. A polymerization mechanism was proposed and a mathematical model for the process was developed.

© 2010 Elsevier B.V. All rights reserved.

1. Introduction

The world production of polymers is about 260×10^6 tons/years. Polyolefins (low density polyethylene, LDPE; high density polyethylene, HDPE; linear low density polyethylene, LLDPE; isotactic polypropylene i-PP; high impact polypropylene, hiPP; and ethylene-propylene rubbers and elastomers, EPDM) account for about 50% of the polymer market.

In spite of their broad use, the presence of olefins in the markets in which the formation of a thin film, well adhered to the substrate surface, is required (e.g., coatings, adhesives) is very limited. These markets are served by solventborne and waterborne polymers, and because of the environmental reasons, waterborne dispersed polymers are gaining share in the market. The presence of water limits the type of polymerization that can be used to synthesize these materials. Waterborne dispersed polymers are mostly prepared by free radical polymerization, which has a limited capability for polymerizing olefins and for controlling the polymer microstructure. Ethylene can be polymerized by free radical polymerization at high pressure [1], but α -olefins cannot be efficiently polymerized by free radical polymerization because the radical formed is too stable.

Catalytic polymerization is extensively used in the production of polyolefins. LLDPE, HDPE, polypropylenes, and EPDM are produced using Ziegler–Natta [2,3], Philips [4] and metallocene cat-

alysts [5–10]. These catalysts allow a good control of the polymer microstructure, but they are based on early transition metals (Ti, Zr, Cr and V), which are oxophilic, and hence very reactive with water. Therefore, they cannot be used in aqueous systems although some success has been obtained by prepolymerizing styrene with metallocene catalysts and dispersing the polymer encapsulated metallocene in water [11]. Late transition metals (Ru, Co, Rh, Ni, Pd) are much less oxophilic and therefore they may be used in aqueous systems. Excellent reviews on the late transition metal catalysts have been published [12–18]. These catalysts were originally developed for solvent-based polymerization and recently have been applied to aqueous systems [19,20].

A pioneering development in late-metal catalysts for ethylene polymerization was the discovery of Keim et al. that neutral Ni complexes of [P,O]-chelating agents were excellent catalysts for the oligomerization of ethylene to short linear α -olefins [21,22]. These catalysts represented the base for the Shell Higher Olefin Process (SHOP), a process which produces primary C₁₁–C₁₅ fatty alcohols for use in detergent industry [23]. The reason of getting short linear α -olefins is that late transition metals are prone to suffer chain transfer by β -hydride elimination [16]. Therefore, much efforts were devoted to develop catalysts able to produce high molecular weight polymers (namely, able to suppress chain transfer) and at the same time maintaining a fast polymerization rate.

Ostoja-Starzewski [24,25] and Klabunde et al. [26] modify the ligand structure of the neutral Ni(II)-P,O based catalysts were able to obtain very high molecular weights ($M_w = 10^6$ g/mol) and high productivities in hexane (TOF = $30,446 \times 10^{-5} \text{ h}^{-1} \text{ Pa}^{-1}$);

* Corresponding author.

E-mail address: jm.asua@ehu.es (J.M. Asua).

where TOF is the turnover frequency defined as

$$\text{TOF} = \frac{\text{mols}_{\text{ethylene-reacted}}}{\text{mols}_{\text{CATused}} \cdot \text{time}(h) \cdot \text{pressure}(\text{Pa})} \quad (1)$$

In addition, the catalysts were active in polar organic media (acetone, DMF and alcohols) [25].

Johnson et al. [27] developed a class of catalyst based on cationic metal (Ni, Pd) complexes of neutral multidentate ligands with nitrogen donor atoms substitutes with bulky groups. Activities of up to $6188 \times 10^{-5} \text{ (h}^{-1} \text{ Pa}^{-1}\text{)}$ and high molecular weights ($>8 \times 10^5 \text{ g/mol}$) were reported. The key feature was the retardation of the chain transfer by the bulky O-aryl substituents. A highly branched polymer, which was attributed to a chain-walking mechanism, was produced. The unique chain-walking characteristics of these catalysts have been used to synthesize a variety of dendritic materials, which could find application as processing aids, rheological modifiers, and amphiphilic core-shell nanoparticles for drug delivery and dye formulation [28,29].

Grubbs et al. [30,31] and Johnson et al. [32] developed a neutral nickel catalysts based on salicylaldimine ligands that yielded moderately branched to linear polyethylenes. Activities up to $13250 \times 10^{-5} \text{ (h}^{-1} \text{ Pa}^{-1}\text{)}$ were reported [31]. These catalysts are active in polar solvents such as ethers, ethyl acetate, acetone and water [31].

Monometallic palladium catalysts containing a sulfonated phosphine ligand chelated to the palladium and a P–C σ bond, which is stable and isolable and contains a weak auxiliary ligand, are particularly promising [14]. A single-pot method to synthesize sulfonic acid phosphine ligands has been developed [33]. Increasing the steric hindrance in the ortho-positions yielded high molecular weights, which was attributed to the bulky substituent blocking at least one of the axial positions on the palladium center.

These catalysts can be effectively used to homopolymerize ethylene or copolymerize ethylene with acrylates [34,35] and a variety of polar monomers including vinyl ethers [35,36], vinyl fluoride [37], N-vinyl-2-pyrrolidone and N-isopropylacrylamide [38].

Skupov [39] studied the performance of a series of palladium catalyst in the solution co(polymerizations) of ethylene and ethylene/acrylates. Very high activities were found for the homopolymerization of ethylene (up to $36,300 \times 10^{-5} \text{ (h}^{-1} \text{ Pa}^{-1}\text{)}$ at 100°C) with high molecular weights ($\overline{M}_n = 133,000 \text{ g/mol}$). The activity decreased rapidly as temperature decreased ($2400 \times 10^{-5} \text{ h}^{-1} \text{ Pa}^{-1}$ at 85°C). The molecular weight increased when the polymerization temperature was reduced ($\overline{M}_n = 156,000 \text{ g/mol}$ at 85°C). The catalysts were able to incorporate acrylates, although the activity strongly decreased with the degree of incorporation of the acrylate.

Claverie et al. [40] showed that the palladium catalysts containing sulfonated phosphine ligands were effective in the homopolymerization of ethylene and the copolymerization of ethylene and acrylates in aqueous media. However, catalyst activity was severely reduced by the presence of both water and acrylates.

Copolymerization of ethylene with vinyl acetate [41], acrylates [42,43] and vinyl sulfones [44] using palladium/alkylphosphine-sulfonate catalysts have been reported. In all cases, incorporation of the polar monomer led to a decrease in the catalyst activity.

The articles reviewed above were mainly devoted to the development of the catalyst. However, the kinetics of the process was mostly limited to the determination of the average turnover frequency (TOF), which gives an idea about the average polymerization rate. Skupov et al. [45] studied the kinetics of the ethylene homopolymerization and copolymerization with acrylates using a sulfonated arylphosphine Pd-based catalyst. Using a kinetic scheme in which the pyridine played a central role, they were able to fit well the effect of the monomer concentration on TOF during the homopolymerization of ethylene. Surprisingly, the kinetic scheme

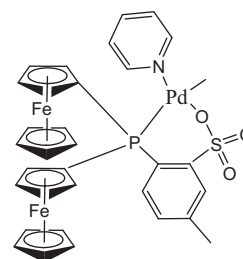


Fig. 1. Catalyst used (provided by Rohm and Haas).

did not consider the coordination of ethylene to the vacant site of the palladium.

This is the first of a series of articles aiming at investigating the kinetics of the catalytic polymerization of ethylene using a monometallic palladium catalyst containing phosphine ligands (Fig. 1). The catalyst was generously provided by Rohm and Haas and it is interesting because it has the potential to be used in aqueous media. The first article is devoted to the polymerization of ethylene in toluene. The effect of temperature, monomer concentration, and catalyst concentration on polymerization rate, polymer molecular weights, polymer architecture and crystallinity was studied. The influence of the diffusional limitations was assessed. The kinetics was analyzed by using a mathematical model and a mechanism for the process was proposed. In a following article, the catalytic polymerization of ethylene in aqueous media will be reported.

2. Experimental

The Pd-catalyst used is sensitive to oxygen, water and other impurities. Therefore, ethylene, nitrogen and toluene were purified. Ethylene (purity 99.9%, $\text{O}_2 < 0.1 \text{ ppm}$) and nitrogen (purity 99.999%, $\text{O}_2 < 0.1 \text{ ppm}$) were further purified in a 3 L-packed column with molecular sieves (13X, 4A and 3A types, Sigma–Aldrich). Toluene purification was performed in two steps. First, it was purged with purified nitrogen at 90°C for 10 h in a system formed by three round bottom flasks in series equipped with condensers. The reason for having three flasks in series was to avoid the diffusion of atmospheric oxygen to the first flask. Then, the toluene from the first flask was introduced in a glove box and passed through an oxygen removal catalyst R3-11 (BASF) with a flow rate of 1 L toluene in 8 h.

Polymerizations were carried out in a 1 L, jacketed, stainless steel Büchi polyclave reactor, able to operate up to a pressure of $6 \times 10^6 \text{ Pa}$ and a temperature of 200°C . An anchor stirrer rotating at 200 rpm was used. The reactor was equipped with two transparent windows and two injection cylinders. It also had entrances for ethylene and nitrogen.

Inside a glove box, the desired amount of catalysts was mixed with 20 mL of clean toluene and sonified for 2 min using a Branson S-450D sonifier (at 10% power). This process helps achieving a good solubilization of the catalyst in toluene. The solution was placed in a 30 mL stainless steel cylinder, which had a valve at each side. The rest of the purified toluene was introduced in a 1 L stainless steel cylinder, which also had a valve at each side. The two cylinders were removed from the glove box and attached to the reactor lid.

Before each reaction, the reactor was pressurized with nitrogen ($20 \times 10^5 \text{ Pa}$) and checked for any leakage by using a soap-water leak detector. The reactor was heated to 100°C and repeatedly pressurized with nitrogen (10^6 Pa), purged and evacuated ($<10 \text{ kPa}$). This operation was performed 10 times to insure an oxygen free system. The toluene contained in the 1 L cylinder was introduced in the reactor by pushing it with nitrogen. The toluene was purged with ethylene at $40 \times 10^5 \text{ Pa}$ during 10 min for nitrogen removal. Then,

the ethylene was evacuated and the system was again pressurized with ethylene at 40×10^5 Pa allowing 10 min for the saturation of toluene in ethylene and for temperature stabilization. Using a nitrogen pressure, the catalyst was injected from the 30 mL cylinder connected to the reactor port. This operation was made trying to minimize the amount of nitrogen entering in the reactor. This started the polymerization. The reactor was sealed and the pressure and temperature recorded. When the pressure in the reactor decreased to about 20×10^5 Pa, ethylene was fed to increase the pressure to 40×10^5 Pa. In some cases, this operation was repeated several times. At the end of the experiment, pressure and temperature were lowered. The polymer was precipitated in 4 volumes of methanol, filtered and dried.

The polymerization in toluene started as a gas/liquid system, but it was observed that the reaction mixture turned milky during polymerization. This indicates that the polyethylene precipitated in the reaction medium. At first sight, this is surprising because the toluene–polyethylene interaction parameter varies from 0.9 at 298 K to 0.4 at 373 K [46]. Therefore, from this point of view, polyethylene is expected to be soluble in toluene at 383 K and it may be soluble at 363 K. The formation of a separate phase may be due to the fact that polyethylene crystallizes at high temperature in good solvents [47–49]. In addition, the reaction medium contained a substantial amount of ethylene (about 2.5 mol/L at 363 K and 40×10^5 Pa) that is a non-solvent for polyethylene and this may reduce the solubility of the polyethylene in the mixture. Therefore, the system evolves to a gas/liquid/solid system as polyethylene is formed. The catalyst may be part of the solid phase, because polymer is formed by coordination polymerization in contact with the catalyst. In such a system, the ethylene should diffuse from the gas phase to the continuous liquid phase (toluene), and then through the continuous phase to the dispersed phase before reaching the catalyst. Therefore, it was necessary to estimate the rate of mass transfer in the system.

A system that has some similarity with the present one is latex devolatilization [50], which is carried out to remove the unreacted monomers (and other volatile organic compounds) from the latex. This is a gas/liquid/solid system in which the mass transfer occurs in the opposite direction (from the solid to the gas through the liquid), but the principles are the same. For latex devolatilization, it has been reported [50] that the mass transfer through the gas/liquid interface is the rate determining step. Taking into account that the latex is stripped with either steam or a water-saturated gas and bubbles are formed, the gas–liquid interface area is larger than in the present case (which is mostly restricted to the upper surface of the reaction mixture). Consequently, the mass transfer of ethylene from the gas to the liquid phase is expected to be the slowest mass transfer process. Therefore, the gas–toluene mass transfer rate was studied. The reactor containing a known amount of toluene (≈ 400 g) was heated to the desired temperature and the ethylene was rapidly fed into the system monitoring both the pressure in the reactor and the ethylene flow rate (Bronkhorst Combi-Flow F1). It was found that the mass transfer rate of ethylene was too fast to be accurately measured at a given pressure. Nevertheless, it was faster than 60 mol/h.

The molecular weight distribution was determined by high temperature gel permeation chromatography (HT-GPC). A Waters-GPCV 2000 instrument equipped with UV and viscometer detectors was used. The polymer was dissolved at 140°C in 1,2,4-trichlorobenzene (with 0.1, w/w Irganox 1010) and passed through a column Styragel[®] HT-Waters of cross-linked polystyrene/divinylbenzene (PS/DVB) particles with a flow rate of 1 mL/min. Polyethylene standards were used for the calibration.

^{13}C NMR spectra were recorded at 130°C in a Bruker Avance 300 MHz spectrometer using 1,2-dichlorobenzene and a pulse delay of 10 s. The signal at 30 ppm corresponding to the methy-

lene backbone was used as reference to determine the position of the rest of the carbons.

The degree of crystallinity was estimated by differential scanning calorimetry (DSC) by comparing the measured melting enthalpy to that of a pure polyethylene crystal. The ΔH_f for a pure polyethylene crystal is estimated to be approximately 280 J/g [51]. A Perkin Elmer Pyris 1 instrument with heating and cooling rates of $10^\circ\text{C}/\text{min}$ was used.

The melting transitions of the polymers are very sensitive to its thermal history. Different crystalline structures are formed depending on the thermal treatment of the sample. The crystallinity data reported corresponded to the second heating cycle.

The morphology of the polyethylene was observed by means of a Hitachi, model S-2700 scanning electron microscope.

3. Results and discussion

In order to evaluate the reproducibility of the process, two reactions were performed at 363 K, using the same catalyst concentration and an ethylene pressure between 40×10^5 Pa and 20×10^5 Pa. The results are presented in Fig. 2 and Table 1. Comparison between the results obtained in runs 1 and 2 show that the polymerizations were reproducible. In addition, the evolution of the reactor pressure indicated that the polymerization rate decreased with time, suggesting that the catalyst deactivated during the process.

The average polymerization rate was 2 mol/h, which is much smaller than the gas–liquid mass transfer rate (>60 mol/h). This indicates that the process was not diffusionally controlled by the mass transfer from the gas phase to the liquid phase. However, this does not mean that the diffusion was negligible because a large amount of polymer accumulated in the reactor. One wonders if this high amount caused mass transfer limitations from the toluene to the catalyst site. In order to determine the reactivity of the catalyst, a shorter experiment (run 3, 1 h) was carried out using higher ethylene pressures (from 40×10^5 Pa to 33×10^5 Pa). The results are given in Fig. 3 and Table 1. It can be seen that a substantial increase of TOF was observed as compared to runs 1 and 2. The higher average ethylene pressure in the reactor was not the reason for this increase because the value of TOF was given by unit pressure. Therefore, it was due to either a higher average catalyst activity (which would indicate the presence of catalyst deactivation) or to a lower diffusional resistance from toluene to the catalytic site (which will be called internal resistance).

In order to investigate the influence of the internal resistance over the polymerization rate at 363 K, a reaction was performed

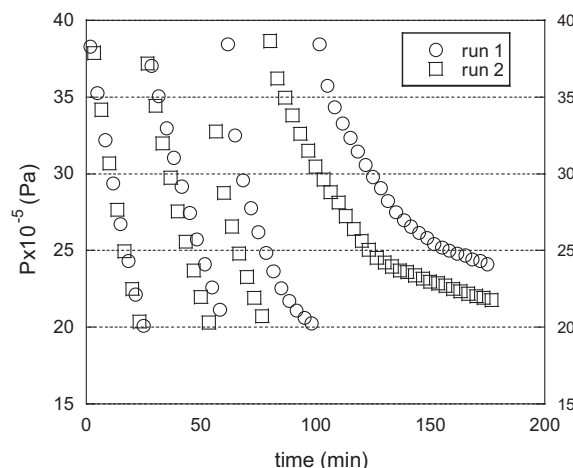


Fig. 2. Evolution of the pressure in the reactor in runs 1 and 2.

Table 1
Summary of the catalytic polymerizations of ethylene in toluene.

Run	Catalyst (mol)	Time (min)	Polyethylene (g)	\bar{P} ($\times 10^{-5}$ Pa)	TOF $\times 10^{5a}$	T (K)
1	4.124×10^{-5}	180	172.8	31.25	1584	363
2	4.124×10^{-5}	180	170	30	1637	363
3	4.124×10^{-5}	60	120.1	36.5	2849	363
4	1.94×10^{-5}	60	70	37	3567	363
5	4.12×10^{-5}	180	25.3	36	204	343
6	4.12×10^{-5}	10	70	34	6427	383
7	1.94×10^{-5}	20	52.2	33.25	8758	383
8	1.03×10^{-5}	20	28.4	37.25	7932	383

^a TOF (mol ethylene \times mol⁻¹ catalyst \times h⁻¹ \times Pa⁻¹).

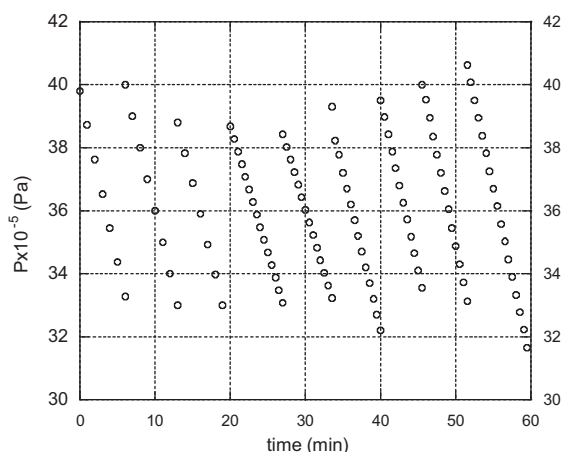


Fig. 3. Evolution of the ethylene pressure in run 3 ($T=363$ K).

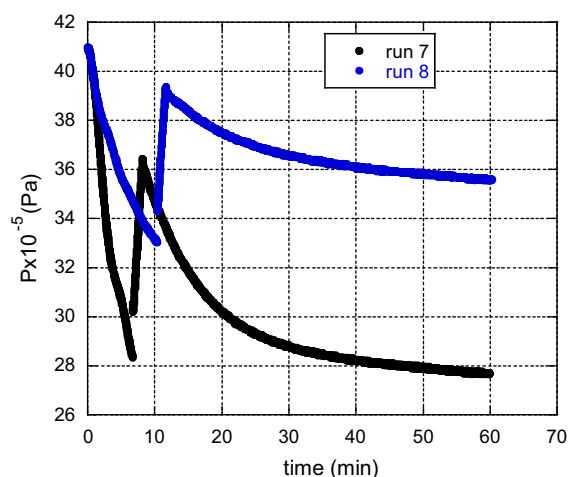


Fig. 5. Evolution of the ethylene pressure in runs 7 and 8 ($T=383$ K).

using less quantity of catalyst (1.94×10^{-5} mol; run 4), obtaining a lower amount of polymer. A value of TOF higher than in run 3 was measured (Table 1). These results strongly indicate that the internal resistance affected the observed polymerization rate.

In order to study the effect of temperature, two polymerizations were carried out at 343 K and 383 K, using the same quantity of catalyst as in runs 1–3. Fig. 4 presents the pressure drop for run 5. Because of the higher heat generation rate, reactor temperature could not be controlled in run 6. In order to achieve a better control of the reactor temperature, two reactions (runs 7 and 8) were carried out with less quantity of catalyst (1.94×10^{-5} mol and 1.03×10^{-5} mol catalyst, respectively). Fig. 5 presents the pressure evolution for runs 7 and 8. Table 1 summarized the results obtained

in runs 4–8. In this table, the TOF value for run 6 was calculated using the first 10 min of the process.

Table 1 shows that the catalyst activity strongly depended on the polymerization temperature. The TOF values for runs 4 and 6–8 were not affected by the gas–liquid mass transfer rate (external resistance) because the overall polymerization rate of 3 mol/h was much smaller than the mass transfer rate from gas phase to toluene (>60 mol/h). It can be seen that TOF decreased and the total amount of polymer increased when higher concentrations of catalyst were used, supporting the hypothesis that the catalyst was less accessible when the amount of polymer increased.

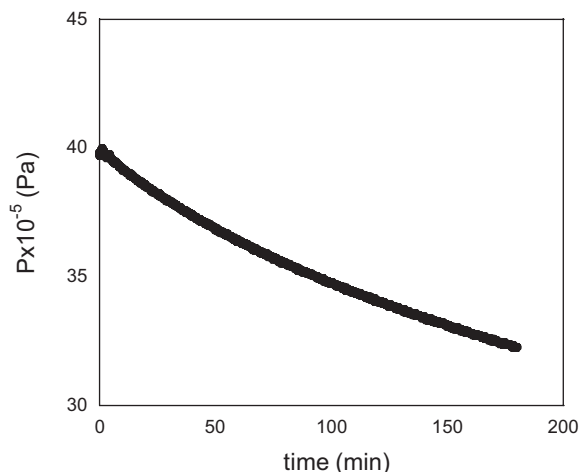


Fig. 4. Evolution of the ethylene pressure in run 5 ($T=343$ K).

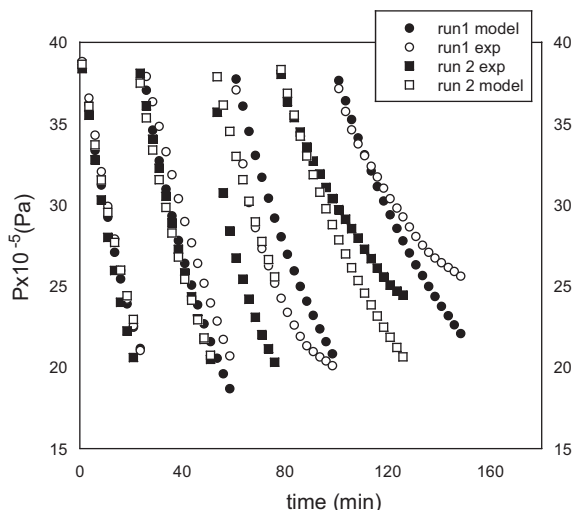


Fig. 6. Experimental values vs. model predictions in runs 1 and 2.

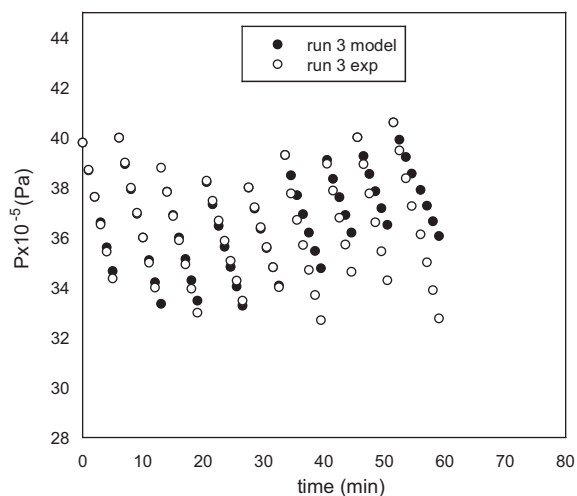


Fig. 7. Experimental values vs. model predictions in run 3.

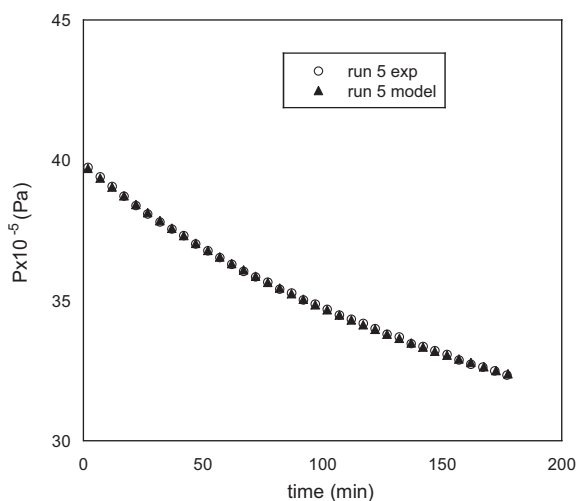


Fig. 8. Experimental values vs. model predictions in run 5.

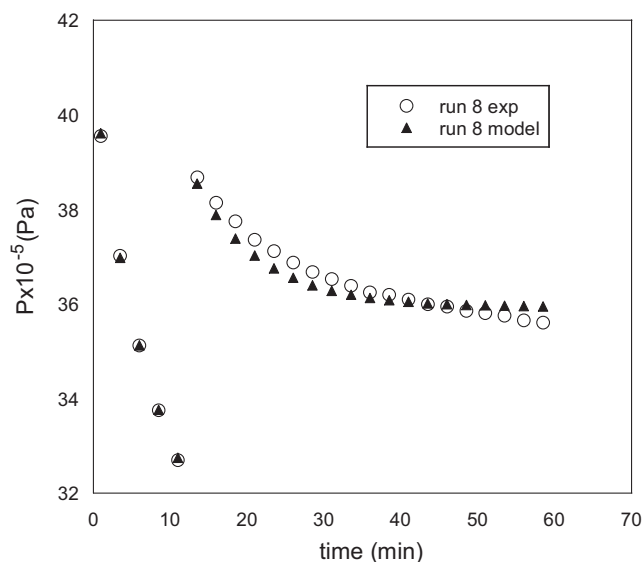


Fig. 9. Experimental values vs. model predictions in run 8.

The deactivation of the catalyst (if any) is a process that would also reduce the polymerization rate during the process. This effect cannot be easily separated from that of the internal resistance to mass transfer of ethylene. Therefore, both processes were pooled together in a rather simplistic way by assuming that the apparent efficiency of the catalyst (a) varied during the process as described in Eq. (3). The mathematical model for the process is:

$$\frac{dE}{dt} = -k_{pEE} \cdot \text{CAT} \cdot a \cdot C_E \cdot V_L \quad (2)$$

$$\frac{da}{dt} = -k_{d1} \cdot a \cdot C_E \quad (3)$$

where E is the ethylene in the reactor (mol), k_{pEE} ($\text{g}^{-1} \text{min}^{-1}$) is the effective polymerization rate constant that includes the effect of the pyridine coordination equilibrium, CAT (g) is the amount of catalyst used in the experiment, a is the apparent catalyst activity ($a = 1$ at $t = 0$), C_E is the concentration of ethylene in the liquid phase,

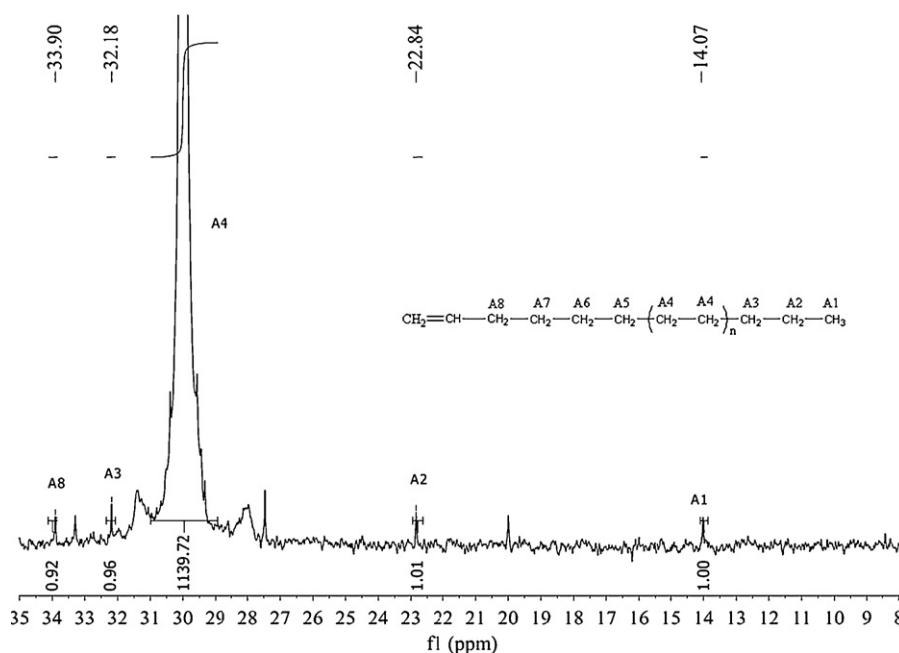


Fig. 10. ^{13}C NMR spectrum of the polyethylene obtained in run 3.

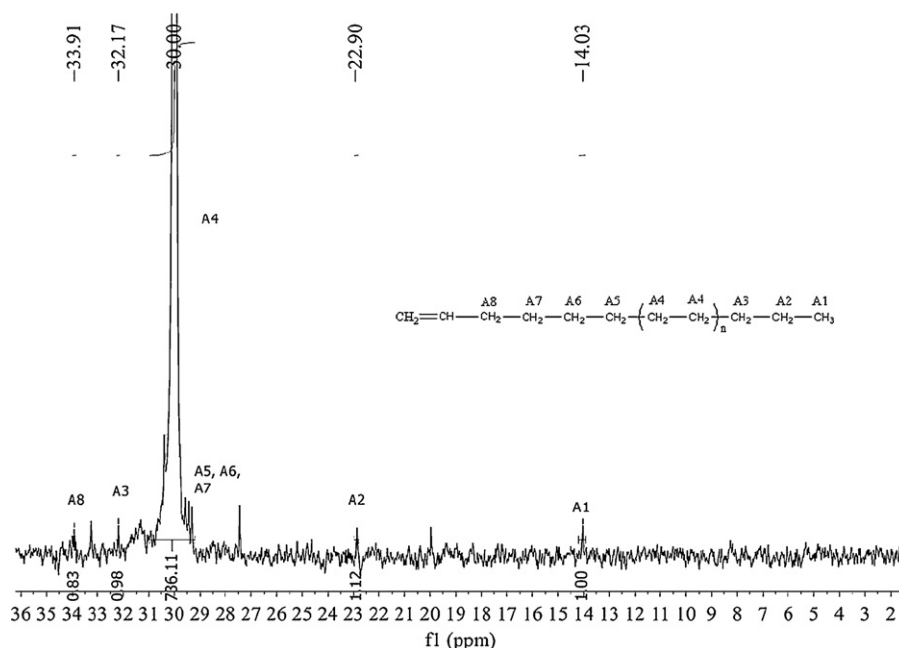


Fig. 11. ^{13}C NMR spectrum of the polyethylene obtained in run 8.

V_L is the volume of the liquid and k_d ($\text{L min}^{-1} \text{mol}^{-1}$) is the so-called deactivation rate constant.

Because the gas–liquid mass transfer ($>60 \text{ mol/h}$) was much faster than the polymerization rate ($2\text{--}3 \text{ mol/L}$), ethylene was assumed to partitioning between the phases according to equilibrium. The Peng–Robinson equation of state (PR EOS) [52] was used to determine the relationship between the pressure and the concentrations of ethylene and toluene in the gas and liquid phases. The binary interaction parameters of the van der Waals mixing rule [53] given by Lee et al. [54] were used in the PR EOS. At time zero, the measured pressure was used as an input to calculate the total amount of ethylene in the system and its concentrations in each phase by combining the PR EOS and the material balances. During the polymerization, the total amount of ethylene given by Eq. (2) was used to calculate the pressure and the concentrations in each phase.

The parameters of the model at the different temperatures were estimated by fitting the evolution of the ethylene pressure in the reactor in runs 1–3, 5 and 8. The estimated values are given in Table 2. Figs. 6–9 show the good fitting of the experimental data. A relatively small deactivation rate constant, which increased with temperature, was estimated and the prediction of the model is that after 1 h at a working pressure between $32 \times 10^5 \text{ Pa}$ and $40 \times 10^5 \text{ Pa}$ at 363 K, the activity of the catalyst was 53% of the initial one.

Table 3 presents the molecular weights of the polymer produced. It can be seen that the molecular weight decreased with temperature. On the other hand, the concentration of ethylene showed almost no effect on the molecular weights as roughly the same molecular weights were obtained in runs 1–3, even though the average monomer concentration in run 3 was substantially higher than in runs 1 and 2. This suggests that chain termination occurred by chain transfer to monomer and that temperature pro-

motes the chain transfer over chain growth. However, dispersity was slightly smaller than the value expected for a chain transfer process ($\text{ĐM} = 2$).

Figs. 10 and 11 present the ^{13}C NMR spectra of the polymer produced in runs 3 and 8, respectively. These figures also present the peak assignment. The number average molecular weight can be estimated from the ^{13}C NMR spectra using the following equation:

$$\overline{M}_{\text{nNMR}} = \frac{A_4/2}{A_1} \cdot 28 \quad (4)$$

The values obtained were $\overline{M}_{\text{nNMR}} = 15,950 \text{ g/mol}$ for run 3 and $\overline{M}_{\text{nNMR}} = 10,300 \text{ g/mol}$ for run 8. These values agreed well with the values obtained by GPC (Table 3). The ^{13}C NMR spectra also showed the presence of terminal double bonds ($-\text{CH}_2-\text{CH}_2-\text{CH}=\text{CH}_2$). For both runs, the number of $\text{CH}=\text{CH}_2$ groups is equal to the number of methyl groups, which suggests that the chain transfer is taking place by β -hydride elimination.

Crystallinity was determined by DSC, using as reference a 100% crystalline polyethylene standard. The crystallinity of the polyethylene obtained was about 80% for all the polymerizations. The

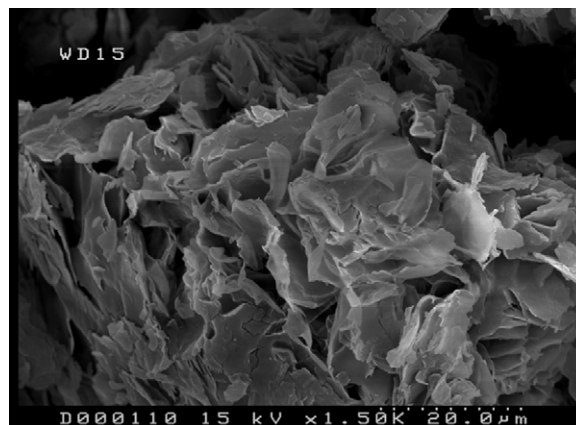


Fig. 12. SEM micrograph of the polyethylene obtained in run 3.

Table 2
Estimated values of the kinetic parameters.

k_{PEE} ($\text{g}^{-1} \text{min}^{-1}$)	k_d ($\text{Lmin}^{-1} \text{mol}^{-1}$)	T (K)
0.078	1.89×10^{-3}	343
1.22	4.6×10^{-3}	363
6.08	5.66×10^{-2}	383

Table 3
High temperature GPC measurements for the polyethylene obtained in toluene.

Run	\overline{M}_n (g/mol)	\overline{M}_w (g/mol)	\overline{DM}	T (K)	Time (h)
1	16269	28980	1.78	363	3
2	15674	27719	1.77	363	3
3	16170	28606	1.77	363	1
5	21316	41637	1.95	343	3
7	8459	15019	1.80	383	1
8	8764	16020	1.83	383	1

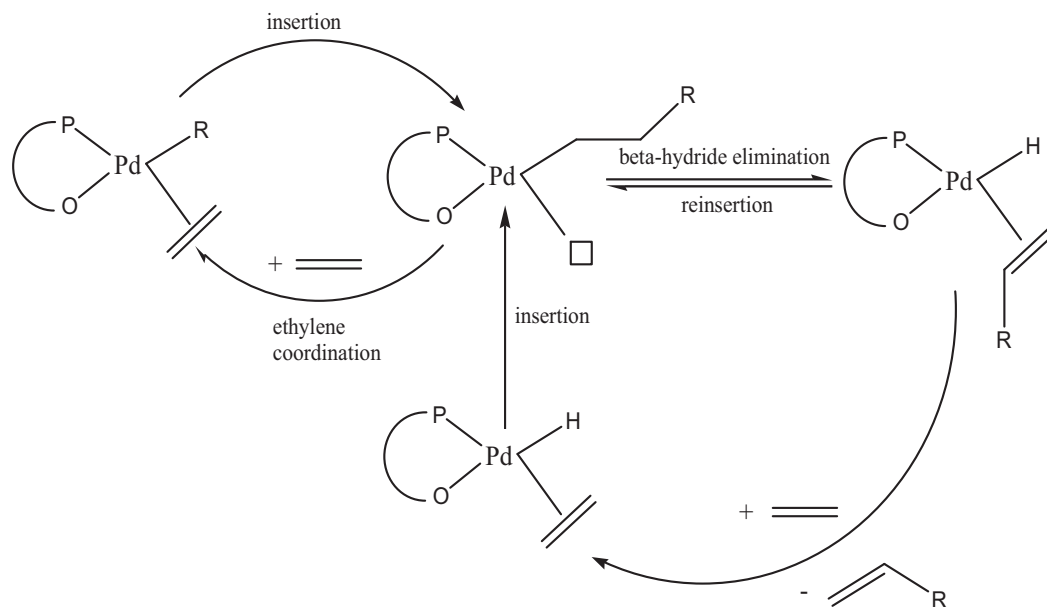


Fig. 13. Proposed mechanisms for the polymerization of ethylene in toluene.

stiffness of the polymer led to the formation of a lamellar structure (Fig. 12).

Fig. 13 presents the scheme of a mechanism that it is consistent with the results obtained. Chain growth occurred by coordination of ethylene to the vacant site of the catalyst followed by insertion. Termination occurred through a β -hydride elimination process; therefore most of the chains contained a terminal double bond. The decrease of the molecular weights with temperature indicated that the activation energy for chain transfer was higher than those of insertion and coordination of the ethylene.

4. Conclusions

The kinetics of the ethylene polymerization of ethylene in toluene using a monometallic palladium catalyst containing phosphine ligands was studied under reproducible conditions. The polymerization rate was much smaller than the gas–liquid mass transfer, namely, the process was not diffusionally controlled by the mass transfer from the gas phase to the liquid phase. However, the reaction was affected by the internal resistance to the mass transfer. The effect of temperature, monomer concentration, and catalyst concentration on the polymerization rate, molecular weights and crystallinity was studied. Polymerization rate strongly increased with temperature but the molecular weights decreased. The so-called deactivation rate constant, which includes both internal resistance and deactivation, increased with temperature. ^{13}C NMR analyses showed that the polymer was mainly formed by linear chains terminated in a double bond at one end and in a methyl group at the other end. This is consistent with a mechanism in which termination occurred through β -hydride elimination. The values of the molecular weights estimated from the ^{13}C NMR spec-

tra agreed well with those determined by GPC. The kinetics of the process was well fitted with the mathematical model developed. The polyethylene obtained had 80% of crystallinity and presented a lamellar morphology.

Acknowledgement

The authors would like to thank Brian Goodall and Lester McIntosh for providing the catalyst. The financial support from Rohm and Haas is gratefully acknowledged.

References

- [1] R.K. Laird, A.G. Morrell, L. Seed, Velocity of ethylene polymerization at high pressures, *Discuss. Faraday Soc.* 22 (1956) 126–137.
- [2] G. Natta, P. Pino, P. Corradini, F. Danusso, E. Mantica, G. Mazzanti, G. Moraglio, Crystalline high polymers of α -olefins, *J. Am. Chem. Soc.* 77 (1955) 1708–1710.
- [3] K. Ziegler, E. Holzkamp, H. Breil, H. Martin, The Mülheim low pressure polyethylene process, *Angew. Chem. Int. Ed.* 67 (1955) 541–547.
- [4] J.P. Hogan, R.L. Banks, Polymerization of olefins, US 2,825,721 (1958).
- [5] W. Kaminsky, The discovery of metallocene catalysts and their present state of art, *J. Polym. Sci.: Part A: Polym. Chem.* 42 (2004) 3911–3921.
- [6] W.E. Piers, T. Chivers, Pentafluorophenylboranes: from obscurity to applications, *Chem. Soc. Rev.* 26 (1997) 345–354.
- [7] A. von Andresen, H.G. Cordes, J. Herwig, W. Kaminsky, A. Merck, R. Mottweiler, J. Pein, H. Sinn, H.J. Vollmer, Halogen-free soluble Ziegler catalysts for the polymerization of ethylene. Control of molecular weight by choice of temperature, *Angew. Chem. Int. Ed. Engl.* 15 (1976) 630–632.
- [8] L. Resconi, S. Bossi, L. Abis, Study on the role of methylalumoxane in homogeneous olefin polymerization, *Macromolecules* 23 (1990) 4489–4491.
- [9] H.G. Alt, S.G. Palackal, W. Milius, Bridged bis(fluorenyl) complexes of zirconium and hafnium as highly reactive catalysts in homogeneous olefin polymerization. The molecular structures of $(\text{C}_{13}\text{H}_9\text{-C}_2\text{H}_4\text{-C}_{13}\text{H}_9)$ and $(\eta^5\text{-}\eta^5\text{-C}_{13}\text{H}_8\text{-C}_2\text{H}_4\text{-C}_{13}\text{H}_8)\text{ZrCl}_2$, *J. Organomet. Chem.* 472 (1994) 113–118.

- [10] M.B. Welch, R.L. Geerts, S.J. Palackal, T.M. Pettijohn, Process and metallocene catalysts for producing polyolefins with broad molecular weight distribution, US 5594078, (1997).
- [11] B. Manders, L. Sciandrone, G. Hauck, M.O. Kristen, No polymerization with metallocene in water? – a prejudice is refuted, *Angew. Chem. Int. Ed.* 40 (2001) 4006–4007.
- [12] S.D. Ittel, L.K. Johnson, Late-metal catalysts for ethylene homo- and copolymerization, *Chem. Rev.* 100 (2000) 1169–1203.
- [13] J.P. Claverie, Catalytic copolymerization in aqueous medium, *Prog. Polym. Sci.* 28 (2003) 619–662.
- [14] B.L. Goodall, Late transition metal catalysts for the copolymerization of olefins and polar monomers, *Topics Organomet. Chem.* 26 (2009) 159–178.
- [15] Z. Guan, C.S. Popeney, Recent progress in late transition metal α -diimine catalysts for olefin polymerization, *Topics Organomet. Chem.* 26 (2009) 179–220.
- [16] S. Mecking, Olefin polymerization by late transition metal complexes—a root of Ziegler catalysts gains new ground, *Angew. Chem. Int. Ed.* 40 (2001) 534–540.
- [17] A. Nakamura, S. Ito, K. Nozaki, Coordination-insertion copolymerization of fundamental polar monomers, *Chem. Rev.* 109 (2009) 5215–5244.
- [18] A. Bekerfeld, S. Mecking, Coordination copolymerization of polar vinyl monomers $H_2C=CHX$, *Angew. Chem. Int. Ed.* 47 (2008) 2538–2542.
- [19] A. Tomov, J.P. Broeyer, R. Spitz, Emulsion polymerization of ethylene and water medium catalyzed by organotransition metal complexes, *Macromol. Symp.* 150 (2000) 53–58.
- [20] A. Held, F.M. Bauers, S. Mecking, Coordination polymerization of ethylene in water by Pd(II) and Ni(II) catalysts, *Chem. Commun.* 4 (2000) 301–302.
- [21] W. Keim, F.K. Kowaldt, R. Goddard, C. Kruger, Novel coordination of (benzoylmethylene)triphenylphosphorane in a nickel oligomerization catalyst, *Angew. Chem. Int. Ed.* 6 (1978) 466–467.
- [22] K. Hirose, W. Keim, Olefin oligomerization with nickel phosphorus–oxygen chelate complexes, *J. Mol. Catal.* 73 (1992) 271–276.
- [23] B. Reuben, W. Harold, The SHOP process—an example of industrial creativity, *J. Chem. Ed.* 65 (1988) 605–607.
- [24] K.A. Ostoja-Starzowski, J. Witte, Highly active ylido-nickel catalysts for the polymerization of ethylene, *Angew. Chem. Int. Ed.* 24 (1985) 599–600.
- [25] K.A. Ostoja-Starzowski, J. Witte, Control of molecular weight of polyethylene in synthesis with bis(ylido)nickel catalysts, *Angew. Chem. Int. Ed.* 26 (1987) 63–64.
- [26] U. Klabunde, S.D. Ittel, Nickel catalysts for ethylene homo- and copolymerization, *J. Mol. Catal.* 41 (1987) 123–134.
- [27] L.K. Johnson, C.M. Killian, M. Brookhart, New Pd(II)- and Ni(II)-based catalysts for polymerization of ethylene and α -olefins, *J. Am. Chem. Soc.* 117 (1995) 6414–6415.
- [28] G. Chen, D. Huynh, P.L. Felgner, Z. Guan, Tandem chain walking polymerization and atom transfer radical polymerization for efficient synthesis of dendritic nanoparticles for bioconjugation, *J. Am. Chem. Soc.* 128 (2006) 4298–4302.
- [29] G. Chen, P.L. Felgner, Z. Guan, Efficient catalytic synthesis of dendritic polymers having internal fluorescence labels for bioconjugation, *Biomolecules* 9 (2008) 1745–1754.
- [30] C. Wang, S. Friedrich, T.R. Younkin, R.T. Li, R.H. Grubbs, D.A. Bansleben, M.W. Day, Neutral nickel (II)-based catalysts for ethylene polymerization, *Organometallics* 17 (1998) 3149–3151.
- [31] T.R. Younkin, E.F. Connor, J.I. Henderson, S.K. Friedrich, R.H. Grubbs, D.A. Bansleben, Neutral, single-component nickel (II) polyolefin catalysts that tolerate heteroatoms, *Science* 287 (2000) 460–462.
- [32] L.K. Johnson, A.M. Bennett, S.D. Ittel, L. Wang, A. Parthasarathy, E. Hauptman, R.D. Simpson, J. Feldman, E.B. Coughlin, Polymerization of olefins in the presence of nickel complexes, *WO 98/30609 A1* (1998).
- [33] N.T. Allen, B.L. Goodall, T.C. Kirk, L.H. McIntosh, Manufacture of ligands useful for polymerization and Heck coupling reaction, US 7,339,075 B2 (2008).
- [34] N.T. Allen, B.L. Goodall, L.H. McIntosh, Single site palladium catalyst complexes having substituted triarylphosphine ligands, US 20,070,287.627 A1 (2007).
- [35] N.T. Allen, B.L. Goodall, L.H. McIntosh, Substantially linear polymers, their manufacture and use, US 20,070,049,712 A1 (2007).
- [36] S. Luo, J. Vela, G.R. Lief, R.F. Jordan, Copolymerization of ethylene and alkyl vinyl ethers by a (phosphine-sulfonate)PdMe catalyst, *J. Am. Chem. Soc.* 129 (2007) 8946–8947.
- [37] W. Weng, Z. Shen, R.F. Jordan, Copolymerization of ethylene and vinyl fluoride by (phosphine-sulfonate)Pd(Me)(py) catalysts, *J. Am. Chem. Soc.* 129 (2007) 15450–15451.
- [38] K.M. Skupov, L. Piche, J.P. Claverie, Linear polyethylene with tunable surface properties by catalytic copolymerization of ethylene with *n*-vinyl-2-pyrrolidinone and *n*-isopropylacrylamide, *Macromolecules* 41 (2008) 2309–2310.
- [39] K.M. Skupov, P.R. Marella, M. Simard, G.P.A. Yap, N. Allen, D. Conner, B.L. Goodall, J.P. Claverie, Palladium aryl sulfonate phosphine catalysts for the copolymerization of acrylates with ethene, *Macromol. Rapid Commun.* 28 (2007) 2033–2038.
- [40] J.P. Claverie, B.L. Goodall, K.M. Skupov, P.R. Marella, J. Hobbs, Novel materials by catalytic polymerization of olefins in emulsion, *Polym. Prepr.* 48 (2007) 191–192.
- [41] S. Ito, K. Munakata, A. Nakamura, K. Nozaki, Copolymerization of vinyl acetate with ethylene by palladium/alkyl phosphine-sulfonate catalysts, *J. Am. Chem. Soc.* 131 (2009) 14606–14607.
- [42] D. Guironnet, P. Roesle, T. Rünzi, I. Göttker-Schnetmann, S. Mecking, Insertion polymerization of acrylate, *J. Am. Chem. Soc.* 131 (2009) 422–423.
- [43] D. Guironnet, L. Caparoso, B. Neuwald, I. Göttker-Schnetmann, L. Cavallo, S. Mecking, Mechanistic insights on acrylate insertion polymerization, *J. Am. Chem. Soc.* 131 (2009) 4418–4426.
- [44] C. Bouilhac, T. Rünzi, S. Mecking, Catalytic copolymerization of ethylene with vinyl sulfones, *Macromolecules* 43 (2010) 3589–3590.
- [45] K.M. Skupov, J. Hobbs, P. Marella, D. Conner, S. Golisz, B.L. Goodall, J.P. Claverie, Kinetic and mechanistic aspects of ethylene and acrylates catalytic copolymerization in solution and emulsion, *Macromolecules* 42 (2009) 6953–6963.
- [46] A.F.M. Barton, *CRC Handbook of Polymer–Liquid Interaction Parameters and Solubility Parameters*, CRC Press, Boca Raton, FL, 1990.
- [47] S.J. Organ, A. Keller, A Solution crystallization of polyethylene at high temperatures. Part 1. Lateral crystal habits, *J. Mater. Sci.* 20 (1985) 1571–1585.
- [48] S.J. Organ, A. Keller, A Solution crystallization of polyethylene at high temperatures. Part 2. Three-dimensional crystal morphology and melting behavior, *J. Mater. Sci.* 20 (1985) 1586–1601.
- [49] S.J. Organ, A. Keller, A Solution crystallization of polyethylene at high temperatures. Part 3. The fold lengths, *J. Mater. Sci.* 20 (1985) 1602–1615.
- [50] R. Salazar, P. Ilundain, D. Alvarez, L.D. Cunha, M.J. Barandiaran, M.J. Asua, Reduction of the residual monomer and volatile organic compounds by devolatilization, *Ind. Eng. Chem. Res.* 44 (2005) 4042–4050.
- [51] J. Brandrup, E.H. Immergut, E.A. Grulke, *Polymer Handbook*, 4th ed., Wiley-Interscience, Hoboken, NJ, 1999.
- [52] D.Y. Peng, D.B. Robinson, A new two-constant equation of state, *Ind. Eng. Chem. Fundam.* 15 (1976) 59–64.
- [53] A. Saraiva, G.M. Kontogeorgis, V.I. Harismiadis, A. Fedenslund, D. Tassios, Application of the van der Waals equation of state to polymers IV. Correlation and prediction of lower critical solution temperatures for polymer solutions, *Fluid Phase Equilib.* 115 (1996) 73–93.
- [54] L.S. Lee, H.J. Ou, H.L. Hsu, The experiments and correlations of the solubility of ethylene in toluene solvent, *Fluid Phase Equilib.* 231 (2005) 221–230.